Supplemental Document

Bifacial-metasurface-enabled pancake metalens with polarized space folding: supplement

Chen Chen,[1,†,2] Xin Ye,[1,†] Jiacheng Sun,[1,†] Yuxin Chen,[1] Chunyu Huang,[1] Xingjian Xiao,[1] Wange Song,[1] Shining Zhu,[1] and Tao Li[1,3,]

[1]*National Laboratory of Solid State Microstructures, Key Laboratory of Intelligent Optical Sensing and Manipulations, Jiangsu Key Laboratory of Artificial Functional Materials, College of Engineering and Applied Sciences, Nanjing University, Nanjing 210093, China*
[2]*e-mail: chenchen2021@nju.edu.cn*
[3]*e-mail: taoli@nju.edu.cn*
[†]*These authors contributed equally to this work.*

Supplement DOI: https://doi.org/10.6084/m9.figshare.21498465

Parent Article DOI: https://doi.org/10.1364/OPTICA.474650

Supplementary Text

Note I: Detailed derivation for electric field response of the supercell

Each meta-atom in the supercell provides polarization-dependent complex amplitude modulation in transmission mode, which can be written as

$$E_1^{\pm}(x,y) = A_1^{\pm}(x,y)\,\mathrm{e}^{\mathrm{i}\varphi_1^{\pm}(x,y)}, \tag{S1}$$

$$E_2^{\pm}(x,y) = A_2^{\pm}(x,y)\,\mathrm{e}^{\mathrm{i}\varphi_2^{\pm}(x,y)}, \tag{S2}$$

where the time-dependence exp(-*iw*$_0$t) is implied, *x* and *y* mark the central position of the meta-atom, and + and - denote a pair of orthogonal states of polarization, which mainly refers to the right and left circular polarized light (RCP/LCP) in this article. If the distance *d* between the adjacent meta-atoms is sub-wavelength scale, the total electric field of the supercell resulting from the collective interference in both *x* and *y* directions can be expressed as

$$E^{\pm}(x,y) = E_1^{\pm}(x,y)+E_2^{\pm}(x,y)=A_1^{\pm}(x,y)\,\mathrm{e}^{\mathrm{i}\varphi_1^{\pm}(x,y)}+A_2^{\pm}(x,y)\,\mathrm{e}^{\mathrm{i}\varphi_2^{\pm}(x,y)}, \tag{S3}$$

where *x* and *y* approximate to the supercell central position. Assuming the transmittance $A_1^{\pm}(x,y) \approx A_2^{\pm}(x,y) \approx 1$, then the transmitted optical field of the supercell can be simplified as

$$E^{\pm}(x,y) = A^{\pm}(x,y)e^{iB^{\pm}(x,y)}, \tag{S4}$$

in which $A^{\pm} = \sqrt{2+2\cos(\varphi_1^{\pm}-\varphi_2^{\pm})}$, and $B^{\pm} = \dfrac{\varphi_1^{\pm}+\varphi_2^{\pm}}{2}$.

Note II: Simulation results of the bifacial metasurface

All utilized supercells have an average simulated transmissivity of 90% and reflectivity of 97% (see Fig. S1). The specific characteristics of a supercell with respect to the wavelength, incident angle and synchronized rotation angle are shown in Fig. S2, indicating a certain robustness and the possibility to combine with PB phase.

The diameter (*D*) of the metasurface is set as 16 μm with numerical aperture *NA*=0.2 in simulations. Figure S3(a) shows the transmitted field profile when illuminated by RCP light through the substrate, termed as forward RCP incidence. The transmittance (*T*) is 81%, and the polarization conversion ratio (PCR), defined as transmitted modulated light power divided by the total transmitted light, is about 94%, shown in Fig. S3(g) and S3(h). The focal length (*f*) is about 34 μm, and the full width at half maximum

(FWHM) of the focus is 1.77 μm. When illuminated by forward LCP wave, as displayed in Fig. S3(b), the light reflects off the surface, showing as a focused OAM beam with l=2, the phase distribution of the OAM focus is shown in Fig. S3(e). Compared with the transmission case, the reflectance reduces to about 63% due to the imperfect destructive interference caused by the neighboring supercells. However, PCR is not affected and maintain a high value as 97%. This kind of spin-dependent metasurface naturally has asymmetric characteristics, as shown in Fig. S3(c) and S3(d), with backward LCP incidence, the light transmits to RCP and focuses to a point, while with backward RCP incidence, the light reflects to form an OAM beam (phase distribution shown in Fig. S3(f)) and maintain the polarization feature.

Note III: Derivation for the phase profiles of bifacial metasurface aimed at pancake metalens

As shown in Fig. S6(a), the marginal light rays are marked as red, and the central rays along the optical axis are marked as blue. The purple ones are the arbitrary middle rays which are first refracted by the metasurface with angle of θ_0 and reflected by the mirror with angle of θ_1 ($\theta_1 = \theta_0$), then are reflected again by the metasurface with angle of $-\theta_2$. According to the geometrical relationship, there comes

$$\begin{aligned} r_2 / r_0 &= R_2 / R_0 \\ r_1 &= \left(r_2 + r_0\right)/2 \end{aligned}, \tag{S5}$$

$$\begin{aligned} \sin\theta_2 &= \frac{-r_2}{\sqrt{r_2^2 + h^2}} \\ \sin\theta_0 &= \frac{r_0 - r_1}{\sqrt{\left(r_0 - r_1\right)^2 + h^2}} \end{aligned}, \tag{S6}$$

in which r_0, r_1, r_2 represent the distance from the position where light ray impinging on the metasurface, the mirror and the metasurface backward again to the corresponding surface center, respectively. Based on the generalized laws of reflection and refraction [1], which can be written as

$$\begin{aligned} \sin\theta_0 &= -\frac{\lambda_0}{2\pi}\frac{d\varphi_0}{dr_0} \\ \sin\theta_2 + \sin\theta_0 &= \frac{\lambda_0}{2\pi}\frac{d\varphi_2}{dr_2} \end{aligned}, \tag{S7}$$

we can obtain the required phase profiles for the light focusing at O_1, as

$$\varphi_T(x,y) = -\frac{2\pi\sqrt{4h^2\left(\frac{R_0}{R_2}\right)^2 + \left(x^2+y^2\right)\left(\frac{R_0}{R_2}-1\right)^2}}{\lambda\left(\frac{R_0}{R_2}-1\right)}$$
$$\varphi_R(x,y) = \frac{2\pi}{\lambda}\left(-\sqrt{h^2+x^2+y^2} + \frac{\sqrt{4h^2+\left(x^2+y^2\right)\left(\frac{R_0}{R_2}-1\right)^2}}{\frac{R_0}{R_2}-1}\right), \quad \text{(S8)}$$

where the value R_0/R_2 equals to the reciprocal of the compression ratio.

In addition to the ray tracing results shown in the manuscript, Figs. S6 (c) and S6 (d) also display the results for the compression ratio of 1/10 and 1/20.

Supplementary Figures

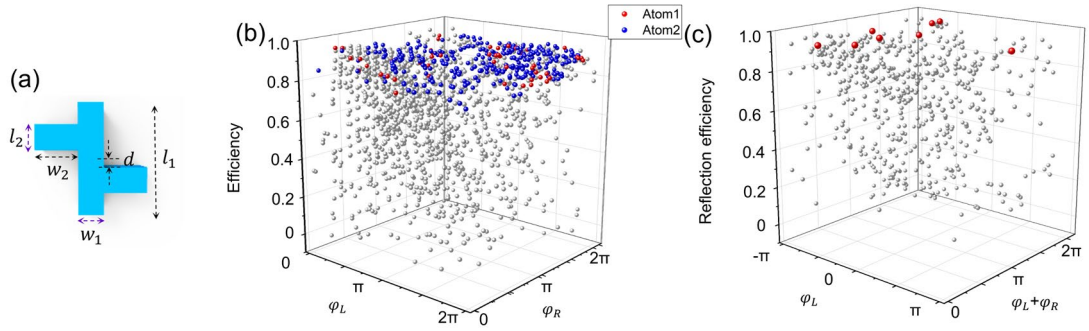

Fig. S1. Two-step design method. (a) The single meta-atom model for geometric parameters sweeping. (b) Simulated cross-polarization conversion efficiency distribution with selected meta-atom pairs marked in red and blue for constructive and destructive interference simultaneously under RCP and LCP incidence. (c) Reflection efficiency distribution of the constructed supercells in (b). Red dots mark the selected supercells with required phase responses.

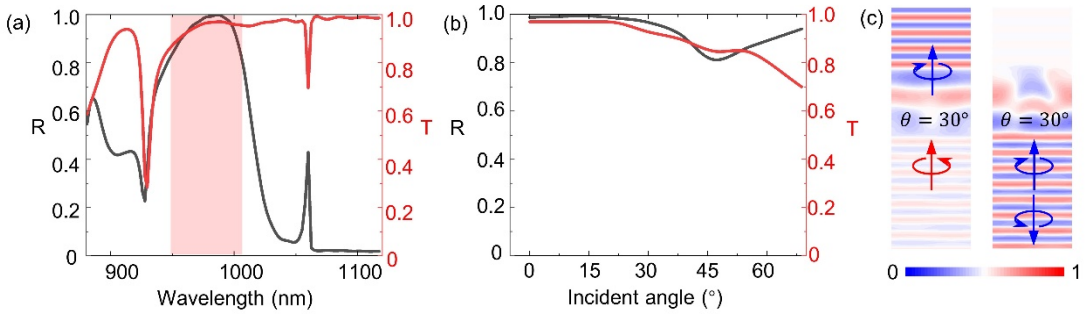

Fig. S2. Characteristics of a supercell. (a) Simulated transmittance and reflectance as a function of wavelength, the colored region indicates a bandwidth of 62 nm (945 nm -1007 nm) with T≥80% and R≥80% simultaneously. (b) Simulated transmittance and reflectance as a function of incidence angle. (c) Electric fields of the supercell with synchronized rotation angle of 30°, the left is $E_x - iE_y$ and the right is $E_x + iE_y$ .The transmittance and reflectance are nearly identical with Fig.2 (b).

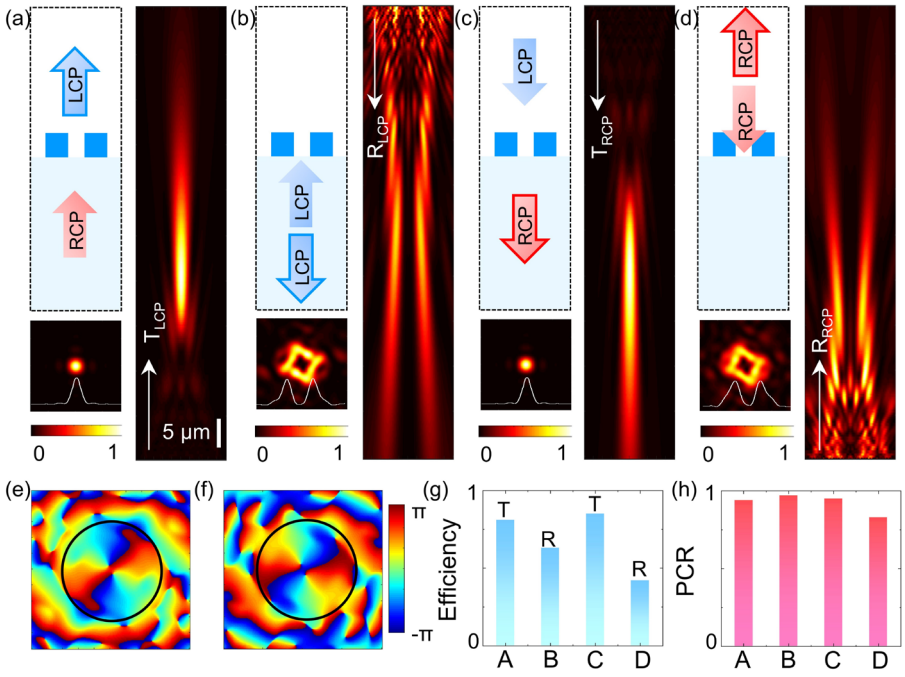

Fig. S3. Detailed simulated results of the bifacial metasurface. Diagram and experimental transmitted/reflected intensity profiles of the metasurface for (a) forward RCP incidence, (b) forward LCP incidence, (c) backward LCP incidence, and (d) backward RCP incidence. Phase distribution of the reflected focused OAM beam with (e) forward LCP incidence and (f) backward RCP incidence. (g) Transmittances and reflectances, (h) polarization conversion ratios in different illumination cases: A, forward RCP incidence; B, forward LCP incidence; C, backward LCP incidence; and D, backward RCP incidence.

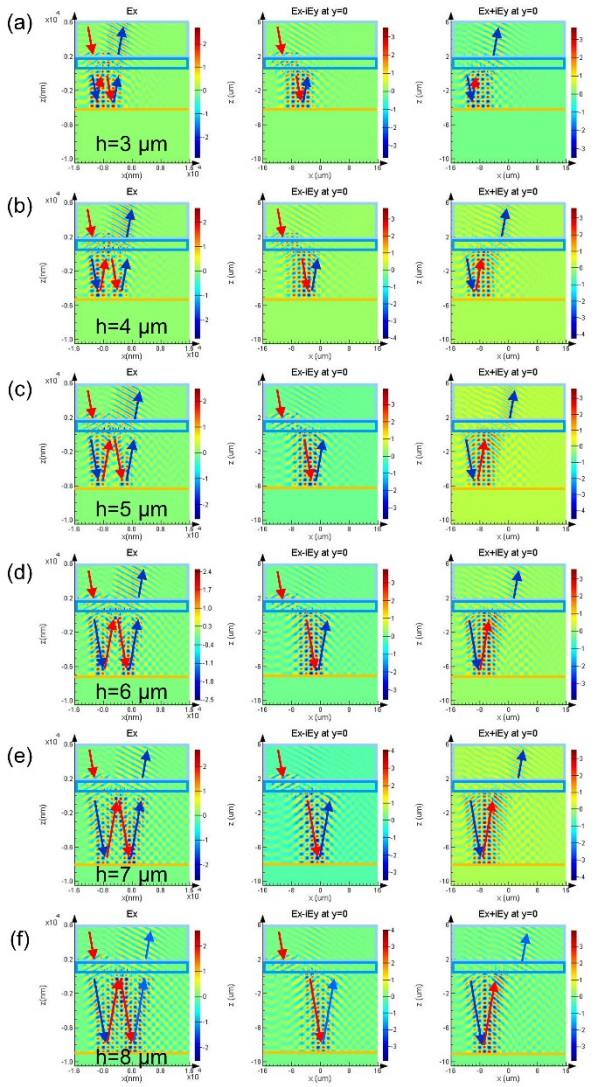

Fig. S4. Electric fields of meta-cavities with different cavity lengths (*h*) under oblique RCP incidence.

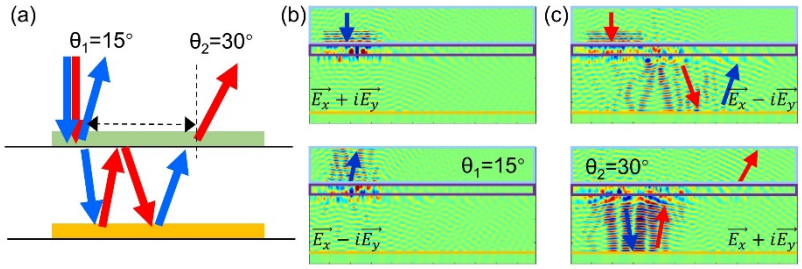

Fig. S5. Spin-dependent reflection angles. (a) Schematic of the shift under normal incidences. Simulated electric fields under normal LCP (b) and RCP (c) incidences with cavity length *h*=9 μm. LCP light is reflected with an angle of 15°, while RCP is reflected with an angle of 30°.

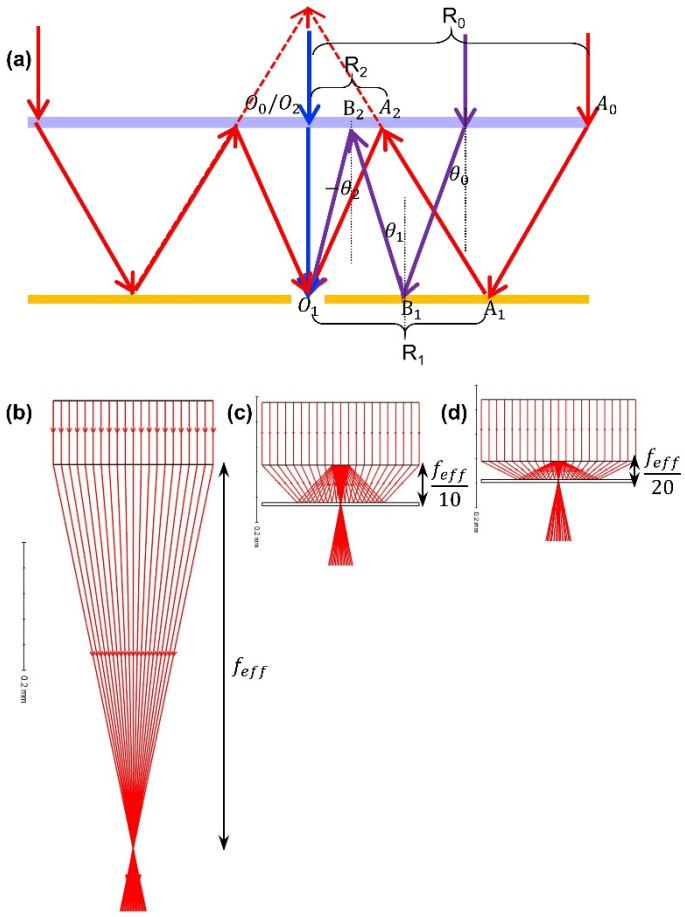

Fig. S6. (a) Schematic of the light rays within the pancake metalens. Ray tracing results for (b) normal metalens, pancake metalens with (c) compression ratio of 1/10, and (d) compression ratio of 1/20.

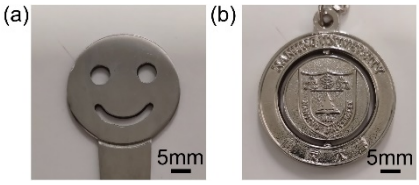

Fig. S7. Photos of (a) a metal spoon handle with happy face shape and (b) a pendant of school badge.

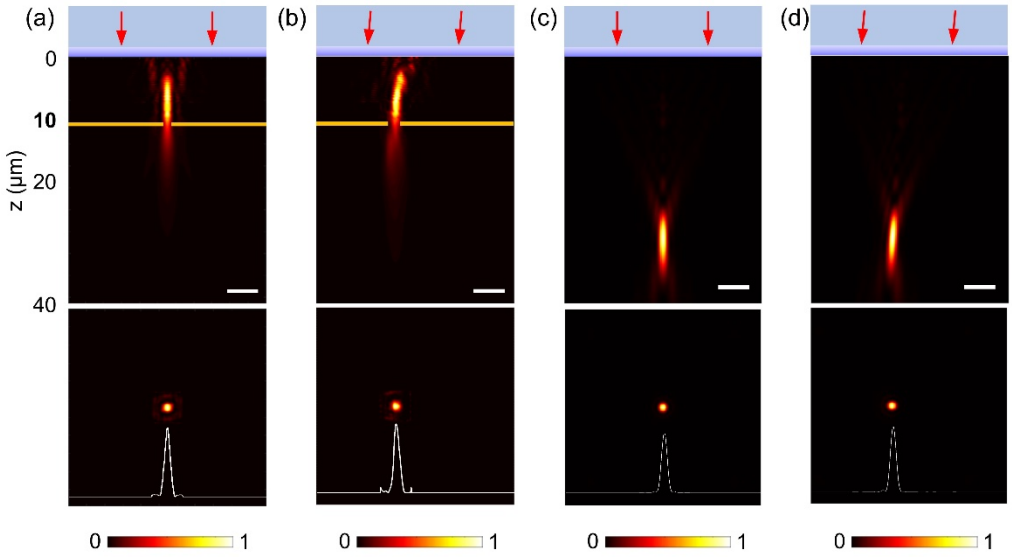

Fig. S8. Focusing performances of the pancake metalens under normal incidence (a) and oblique incidence (5°) (b). Corresponding results of the normal metalens under normal incidence (c) and oblique incidences (d). The focus of pancake metalens shifts about 3 μm compared to normal incidence and deviates from the central hole, which would be blocked if the central hole is not large enough. While if we increase the size of the central hole, the intensity of the light which can be modulated will decrease. The hole size effect will not happen to normal metalens, where the focus shifts about 2.7 μm and can be detected without block.

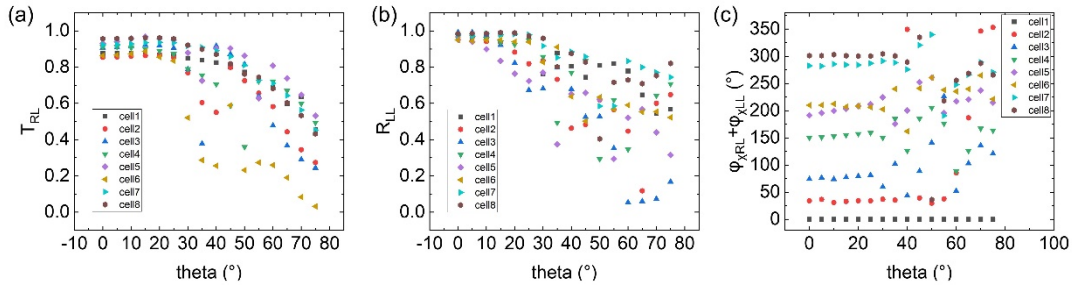

Fig. S9. Simulation results of the picked supercells with different incident angles (theta). (a) The transmissivity of LCP light with RCP incidence. (b) The reflectivity of LCP light with LCP incidence. (c) The total phase shifts including both the transmission and reflection parts. When the incident angle increases to about 40°, the modulated transmissivity and reflectivity, and the total phase shifts start to deviate from the presupposed values, which will limit the minimum value of CR.

Table S1 Geometric parameters of the final picked supercells (unit: nm).

atom one-l_1	atom one-w_2	atom one-d	atom two-l_1	atom two-w_2	atom two-d
280	60	-60	190	60	15
160	80	0	280	60	-10
280	70	-10	160	80	0
250	50	-25	240	110	-120
220	120	-50	210	70	-105
320	70	-60	200	80	20
160	70	0	270	50	-15
160	70	0	270	50	5

Table S2 Maximum incident angle to the pancake metalens with respect to the NA and CR.

NA / CR	0.1	0.2 (experiments)	0.3	0.47 (simulations)	0.62
1/3	6°	11°	17°	27°	38°
1/4	9°	17°	25°	38°	**49°**
1/5	12°	22°	32°	**46°**	
1/6	14°	27°	38°		
1/7	17°	31°	**43°**		
1/8	20°	35°			
1/9	22°	39°			
1/10	25°	**42°**			
1/15	36°				
1/20	**44°**				

For pancake metalens with NA=0.1, 0.2, 0.3, 0.47, and 0.62, the maximum incident angle to the reflection modulation surface will exceed 40° when CR reaches 1/20, 1/10, 1/7, 1/5 and 1/4, respectively. Therefore, the minimum value of CR for pancake metalens with above NA could be inferred to ~ 1/20, 1/10, 1/7, 1/5 and 1/4, correspondingly. Among them, the results for NA=0.47 is also in accordance with the current simulations (Fig. 4(g)), the working distance can be compressed

to 1/5 while with deteriorated quality because part of the incident angle exceeds 40°.

References

1. Yu, N. et al. Light propagation with phase discontinuities: generalized laws of reflection and refraction. *Science* **334**, 333–337 (2011).